NASA TT F-10,171

YIELD MEASUREMENTS ON COLLISION OF SLOW ELECTRONS WITH INERT GAS ATOMS

H.Maier-Leibnitz

FACILITY FORM 602

N66 28583 (ACCESSION NUMBER)

(THRU)

41 (PAGES)

1 (CODE)

(NASA CR OR TMX OR AD NUMBER)

24 (CATEGORY)

Translation of "Ausbeutemessungen beim Stoss langsamer Elektronen mit Edelgasatomen". Zeitschrift für Physik, Vol.95, pp.499-523, 1935.

GPO PRICE $ _____

CFSTI PRICE(S) $ _____

Hard copy (HC) 2.00

Microfiche (MF) .50

ff 653 July 65

NATIONAL AERONAUTICS AND SPACE ADMINISTRATION
WASHINGTON JUNE 1966

YIELD MEASUREMENTS ON COLLISION OF SLOW ELECTRONS WITH INERT GAS ATOMS

*/499

H.Maier-Leibnitz

28583

The excitation of helium, neon, and argon by electron collision is investigated by an electric multiple collision method. Two procedures are described for measuring, at low electron velocities, the total yield during a collision, i.e., the excitation probability of all terms, with sufficient accuracy. The results on total yield are practically free of instrument errors and have an accuracy of 20%. Excitation and ionization yields were separated by ionization probability measurements. Yields of several percent were obtained. Various statements are made on the excitation functions of individual terms. Rather sharp maxima of yield are obtained within 1 v above the excitation potential.

The quantitative study of the transfer of energy during collision of electrons with atoms has made considerable progress in recent years. Specifically, the elastic and inelastic scattering during a single collision and the variation in yield of exciting collisions with the velocity have been investigated. In addition, quantitative statements on the collision process were formulated on the basis of wave mechanics, which mostly agreed with experimental results. Nevertheless, a considerable gap remains in these measurements and calculations: In the direct vicinity of the critical potentials, both experiment and theory

---

* Numbers in the margin indicate pagination in the original foreign text.

furnish rather unreliable values. Older qualitative measurements, which were used in the determination of critical potentials, apparently indicated that a relatively large yield is obtained at each jump, directly behind the excitation potential. Conversely, most measurements on optical excitation functions pointed toward a gradual rise over a range of at least 5 - 10 v.

For the theory, the aspect of the excitation functions near the critical potentials is of interest since, because of the long residence time of the knock-on electron in the atomic union, considerable perturbations of the atomic field are created; this leads to processes that differ from those in the case of fast electrons where extensive analogy with the absorption of light quanta exists. For an application of the results to the discharges of dilute gases, it is exactly the yield at low electron velocities that is of importance, especially if one is successful in measuring the total yields for excitation and in comparing these yields with those for ionization.

Sponer (Bibl.1), in an investigation on mercury, was the first to use /500 a method based on experimental setups that had previously been used for the determination of excitation potentials. Later, Seiler (Bibl.2) used the same experimental method in a more refined version. It was found that the method permits a satisfactory coverage of the low velocities and a simple determination of the absolute yields. Our investigation was conducted in continuation of these studies. In addition, we refined the experimental method. Special emphasis was placed on detecting all error sources, so as to obtain final results of high accuracy.

1. Description of the Apparatus

Figure 1 shows a schematic sketch of the setup used. Its layout had been

furnished by Harries (Bibl.3). This author and, later, Ramien (Bibl.4) used the described arrangement for determining the transfer of oscillatory energy during electron collisions in molecules. Seiler measured yields for the case of mercury. The layout is rotational-symmetric. Electrons, emitted by the filament wire at the center, are accelerated by a field between the filament and the inner cylinder and, in part, enter the collision space through the slit. The collision space itself is field-free. The electrons, under numerous collisions with the filling gas, diffuse in part toward the outer cylinder where they are able to reach the collector through a grid. An arbitrary number of opposing fields can be placed between collision space and collector, for analyzing the stream of incident electrons.

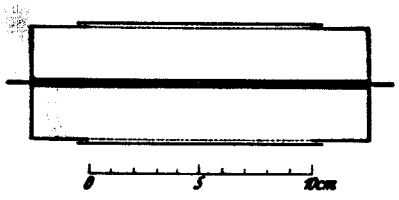

Fig.1 Schematic Sketch of the Experimental Setup

The practical design was very similar to that used by Ramien and Seiler. The collision volume consisted of two coaxial cylinders of 1.5 and 25 mm radius. The length of the collision volume was 150 mm. The electrons emerged from the inner cylinder through a slit of 0.2 mm width. The electron source was a tungsten single crystal of 0.12 mm diameter. The major part of the surface of the outer cylinder was formed by a wire grid of 0.25 mm mesh, with the collector installed behind this grid at a distance of 1.5 mm. The collector was sealed off from the collision volume by quartz crystal, while the filament was sepa- /501 rated from it by hard glass. All metal parts were made of copper. The entire arrangement was blown into a hard-glass tube, so that no ground joints or

cemented seams were necessary. To prevent oxidation of the copper during the blowing process, the tube was rinsed with a stream of nitrogen. After installation, the tube was baked in the conventional manner at a temperature slightly above 400°C and reduced in hydrogen. Criteria for completely reliable conditions comprised full maintenance of vacuum on standing and the disappearance of all contact potentials, which was attained at complete reduction. The installed tube was protected from vapors by attaching a continuously cooled gas trap.

The circuitry was of the conventional voltage-divider principle. Both the accelerating potential and the countervoltage were tapped from the same battery. The collector current was measured with a galvanometer whose sensitivity was 10^{-9} amp per scale division. Occasionally, an instrument with a 20 times greater sensitivity was used. The emission itself was measured with a second galvanometer. For measuring the Hertzian difference curves (see p.6) as well as for adjustment of a constant ratio of accelerating potential to countervoltage, simple auxiliary devices were installed for facilitating the measurements. A part of the countervoltage curves were recorded with a simple apparatus. The slide-wire of a high-quality resistance was directly coupled with the feed of the recording chart. Thus, the displacement was always proportional to the countervoltage, while the galvanometer deflection was reproduced in the other coordinate. As voltage marks, light spots were imprinted. The setup, despite its simplicity, operated satisfactorily and saved a great deal of time.

In general, we worked with collector currents of about $2 - 5 \times 10^{-8}$ amp (in the sensitive instrument, about 10 times less). The velocity distribution was not the same for all filaments and fluctuated between 0.7 and 1.0 ev half-width. At a half-width of 1 ev, the mean energy of the electrons was by about 0.5 ev higher than the accelerating potential.

2. General Principles of the Experimental Method

For mercury, Seiler derived the yields from evaluating the countervoltage curves. Briefly, the procedure is as follows: The primary electrons, entering the collision space, reach the collector in a reduced number and, in part, /502 at a reduced velocity. The number is reduced by back-scattering to the inner cylinder and by losses at the grid and sidewalls of the collision space. The velocity is reduced by inelastic collisions with the gases to be measured. Seiler made the assumption that the diffusion loss, for electron groups of different velocity, was percentagewise equal. From an analysis of the countervoltage characteristics, he determined the relative number of fast and slow electrons, after their passage through the collision space, and calculated the yields from this. However, if slow and fast electrons have differing mean free paths and if the number of collisions is high, the diffusion losses will differ and the method will lead to considerable errors. A more general method will have to take this into consideration. It was found that this can be done in a simple manner only for electrons that traverse the collision space without energy loss. The stream of such electrons, reaching the collector, is reduced not only by the diffusion losses but also by the inelastic collisions. Allowance for its variation with the pressure and with the accelerating potential will make it possible to eliminate the diffusion losses. The losses by inelastic collisions are used for determining the yield. With this method, the total yield can be measured, i.e., the probability that, during a collision, some quantum transition is excited.

The method will be discussed in more detail below. The following quantities can be measured: the current A reaching the collector; the current E collected on the inner cylinder and on the walls of the collision space; the accele-

rating potential V; the countervoltage U; the pressure p of the gas. The emission E constitutes a criterion for the current entering the collision space, since this current is proportional to E, provided that E is large with respect to A and provided that no noticeable perturbations by collisions occur in the accelerating field. Since the diffusion of the electrons is independent of their number so long as no space charges are generated, the quotient A/E, at low currents, will be independent of E. Consequently, the "reduced collector current" A/E is uniquely determined in each gas by the three quantities U, V, and p, independent of the emission of the hot wire. Therefore, in the evaluations, only A/E was used and designated simply as "collector current I". If the pressure is left constant for the time being, the collector current can be generally represented by an area above the UV plane. The curves V = const, on this area, are the countervoltage characteristics as plotted by Seiler. However, in Seiler's results, one factor for each curve is indeterminate since he did not measure the emission. The curves U = 0 are current-voltage characteristics as they were frequently measured in earlier investigations (Bibl.5). The dif- /503
ferences of the curves U = 0 and U equal to a low voltage (for example 0.2 v) were used by Hertz (Bibl.6) for an accurate determination of critical potentials.

For discussing the current area, we will begin with the countervoltage curves whose properties had been discussed already in detail by Harries, Ramien, and Seiler. For the time being, we will speak only of such countervoltage curves as they are formed by electrons of uniform energy. The characteristic slope of these curves results from the directional distribution of the electrons entering the counterfield, and is modified by various factors. These factors primarily include: inhibition of the various electron directions by the grid; curvature of the electron trajectories in front of the grid due to transcon-

ductance of the counterfield; perturbation by collisions in the counterfield. A calculation of the slope of the countervoltage curves, under consideration of the various factors, is impossible; nevertheless, Harries was already able to demonstrate that the countervoltage curves in the various gases and at differing electron velocities are "similar" so long as the mean free path is equal. Even at differing mean free path, the similitude is approximately maintained. Here, the term "similar" means that two curves of differing electron energy can be transformed into each other by affine distortion. Consequently, we have

$$i/i_0 = f\left(\frac{U}{V}\right),$$

if i_0 denotes the collector current at a countervoltage of zero. A negligible impairment of this similarity may be produced by a difference in the variation of the mean free path during the radiative stopping. Of importance is still another perturbation, occurring at higher electron velocities, namely, the perturbation by reflections at the collector. This might lead to variations up to 20%; predominantly, the values at low countervoltages are strongly influenced. In this case, the evaluation method, used by Seiler, would result in errors up to 50%.

As a typical example, Fig.2 shows an experimentally measured countervoltage characteristic. The curve was plotted for helium at an electron velocity of 17.5 ev; therefore, no inelastic collisions occur as yet.

Until now, we only considered the case that electrons of uniform velocity /504 enter the counterfield. If also inelastic collisions take place in the collision space, also slower electrons will enter this field. This will lead to a composite countervoltage characteristic. This curve simply is the sum of the countervoltage curves of the various components, at the ratio at which these are present in the collision space almost in front of the grid. Figure 3

shows such a composite countervoltage characteristic, plotted for argon at 14.0 ev. The same diagram also gives the graphic separation of the three components of 14.0, 2.5, and 1.9 ev. This method was used by Seiler for evaluating his measurements in mercury.

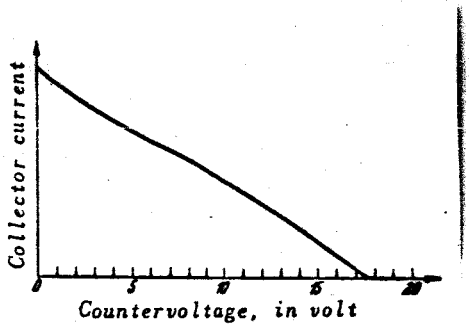

Fig.2 Countervoltage Curve in Helium at 17.5 ev

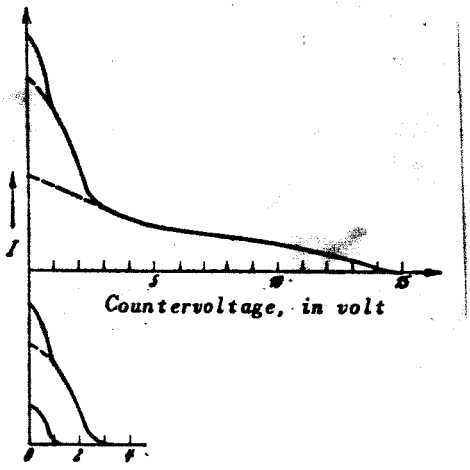

Fig.3 Countervoltage Curve in Argon at 14.0 ev

The finite width of the energy distribution, which had been neglected until now, also manifests itself in a superposition of various countervoltage curves. It is obvious that this will affect the slope only at the very tip of the curves. The situation is different in electrons that had undergone inelastic collisions and whose energy frequently is no longer high in comparison with the width of the energy distribution of the primary electrons. In this case, the slope of the excitation function also has an influence on the form. This will be dis-

cussed later in the text.

3. Diffusion Processes in the Collision Space; Determination of Total Yields from Current-Voltage Characteristics

To understand why, for example, at a countervoltage of zero the collector current varies with the accelerating potential, the diffusion process in the collision space must be considered in somewhat more detail. For this, we /505 will use the diffusion theory developed by Hertz (Bibl.7). For the mathematical treatment, we will assume that the influence of the sidewalls can be neglected; consequently, we let these walls shift into infinity and consider the case of two infinitely long coaxial cylinders with the radii r_0 (inner cylinder) and r_a (outer cylinder). In addition, we will assume that the entire inner cylinder emits electrons, rather than only a narrow slit on this cylinder as is the case in reality. Since the diffusion of the electrons takes place entirely independently, the two cases are fully equivalent. Finally, for a simple treatment it is necessary to assume that the electrons are emitted by the inner cylinder not only in a vertical direction but also uniformly in all possible directions. The resultant errors were exhaustively discussed in a paper by Bartels and Nordstrom (Bibl.8). The errors are small so long as the number of collisions is sufficiently large.

The diffusion equation, for the case in question, reads

$$i(r) = -\frac{v\lambda}{3}\frac{d\varrho}{dr},$$

where i denotes the current density, ϱ the charge density, v the velocity, λ the mean free path of the electrons, and i_a the current incident on the outer cylinder per unit area. The continuity condition is

$$ir = i_0 r_0 = i_a r_a.$$

For the charge density ρ, considering that the charge density at the collector, i.e., at $r = r_a$, must be zero, the following expression is obtained:

$$\frac{A}{r_a} \ln \frac{a\gamma}{r_i \varepsilon_0} = 0$$

Of the electrons distributed in this manner over the collision space, only a portion reaches the outer cylinder, while the remainder diffuses toward the inner cylinder and is lost to the current measurement. The emission current, originally emitted per centimeter length of the inner cylinder envelope, thus is the sum of the current A reaching the corresponding area of the collector and the current of the back-scattered electrons I_r:

$$E = A + I_r = 2\pi i_a r_a + 2\pi i_r r_a$$

The current density of the back-scattered electrons will be

where ρ_0 denotes the charge density at the inner cylinder and $\bar{v}$ the mean velocity component of the incident electrons in a direction perpendicular to the cylinder. We have /506

$$\bar{v} = \frac{v}{4\pi} \int_0^{\pi/2} 2\pi \sin\varphi \cos\varphi \, d\varphi = \frac{v}{2},$$

i.e.,

$$i_r = \frac{3 i_a r_a}{2\lambda} \ln \frac{r_a}{r_0}$$

and

$$E = A\left(1 + \frac{3 r_0}{2\lambda} \ln \frac{r_a}{r_0}\right).$$

Consequently, the collector current will be lower the shorter the mean free path of the electrons. The losses calculated in this manner are relatively high; for example, according to this calculation and at a mean free path of 1.5 mm, only one third of the emission will reach the collector, if the cylinder radii of the experimental setup are used as basis. The real losses will be even larger,

since pressure-dependent losses occur also along the walls and at the portion of the outer cylinder which has not been designed as collector. Figure 4 shows the experimentally plotted variation in collector current with pressure, as it occurs in argon for electrons of 10.5 ev.

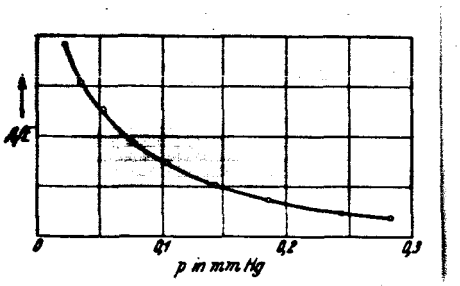

Fig.4 Collector Current as a Function of Pressure; Argon at 10 ev

The reason for the fact that the current, in current-voltage characteristics, is not constant is entirely obvious. The upper portion in Fig.5 shows a curve for U = 0 in helium, at a pressure of 0.326 mm Hg. As long as no inelastic collisions occur, i.e., up to about 19 ev, the current slope can be explained by the mean free path which varies with the electron velocity. Above 19 ev, the diffusion of fast and slow electrons becomes superposed. Since the slow electrons are produced only in the collision space by inelastic collisions, their losses will obey laws different from those for primary electrons, except in the simplest case in which the mean free paths are equal in both cases. /507 Consequently, it will be impossible, even at known yield of inelastic collisions, to make a quantitative prediction as to the slope of the curve and, just as little, to estimate the yield from the measured slope. The situation changes as soon as current-voltage characteristics are used at countervoltages at which only fast electrons are able to reach the collector. Here, it is advisable to use a countervoltage equal to a constant fraction of the accelerating potential,

in which case the factor must be so selected that, at the maximum electron energy entering the measurement, the countervoltage is still sufficient for inhibiting the fastest electrons produced by inelastic collisions. By maintaining U/V constant, the "similarity" of the countervoltage curves can be utilized. This results in the lower curve in Fig.5. Below 19 ev, the slope is similar to that of the upper curve at a countervoltage of zero. Thus, it can be stated that the curve U = V/3 shows the influence of the mean free path in a more accurate form since, at such a countervoltage, the influence of the perturbing reflections is much less noticeable.

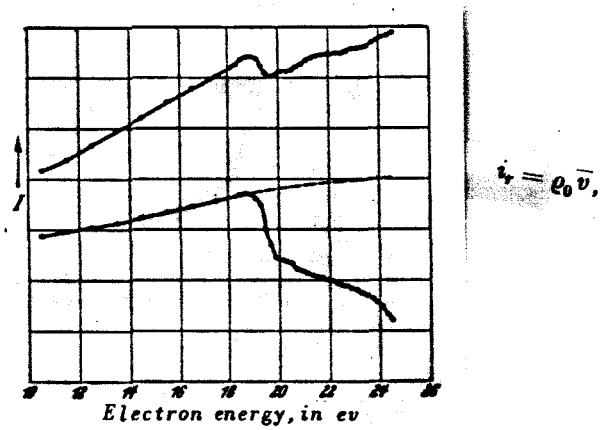

Fig.5 Current-Voltage Characteristics in Helium at 0.326 mm Pressure
Upper portion, countervoltage U = 0; lower portion ("test curve"), U = V/3.

If no inelastic collisions were to occur above 19 ev, the curve would continue along the broken line. This curve, with the aid of the effective cross section curve of helium, is obtained either through Fig.4 or through direct extrapolation from the slope below 19 ev. In the latter procedure, it is assumed that, within the rather narrow range in question, the curve in Fig.4 can be approximated by an exponential curve. This is actually the case. Consequently, this simple method has come into general use.

The drop in experimental values with respect to this "elastic curve" can be due only to a decrease in the number of fast electrons by inelastic collisions. If the current, in the absence of inelastic collisions, is I_{el} then a current of $I_{el} e^{-\eta n}$ will remain after n collisions. Here, η denotes the probability that an inelastic transition takes place during a collision, i.e., the /508 total yield for a single colli- ...otal yield, over the simple relation

$$\ln I_{el} - \ln I = \eta n$$

thus follows direc...y from I, I_{el}, and from the number of collisions n. This evaluation method is characterized by great principal simplicity and has been applied with excellent results. Its special advantage lies in the fact that it accurately furnishes the slope of the total yield. The minor break in the curve of Fig.5, at a value of 20.7 ev, no doubt is real and occurs in all curves.

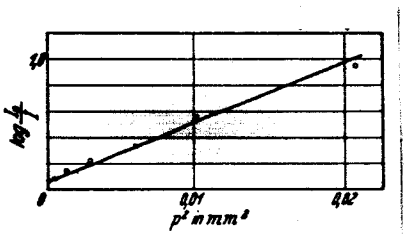

Fig.6 Yields as a Function of the Square of the Pressure; Argon at 12.5 ev

To give an idea on the accuracy of the absolute values, the course of ηn is plotted in Fig.6 as a function of the number of collisions, as a typical example. The slope of the curve (in the diagram, to within a factor) indicates the excitation probability η. The deviations, noted at a low number of collisions, most likely are systematic errors committed in plotting the "elastic curves", which become especially apparent in the case of low yields. At increasing yields, this error gradually starts entering only proportionally. The fact that the straight line does not go through zero can be tolerated since

also the neutral point is influenced by an error of the elastic curve. The error of η, i.e., of the slope of the fitting curve, presumably will be about 10%. To this must be added the mean-square error from the determination of the number of collisions.

4. Remarks on the Number of Collisions

Harries and Hertz (Bibl.9), based on the Hertzian diffusion [illegible] slow electrons, calculated the number of collisions [illegible] by electrons of known mean free path between two coaxial infinitely long cylinders. The formula reads

$$n = \frac{3}{4}\frac{r_a^2}{\lambda^2}\left(1 + \frac{r_0^2}{r_a^2} - \frac{1 - \frac{r_0^2}{r_a^2}}{\ln \frac{r_a}{r_0}}\right).$$

The main postulates of the diffusion theory enter into this formula. The first postulate stipulates that the dimensions of the apparatus must be large with respect to the mean free path of the electrons. The second postulate stipu- /509 lates that the scattering probability in an individual collision is equal for all angles, i.e., that the atoms reflect like elastic spheres.

The deviations produced by the first postulate at low pressures were discussed by Bartels and Nordstrom (Bibl.8) for the simple case of two plane plates. If these considerations are applied to the present case, it will be found that the error, down to about 10 collisions, will not be greater than 15%. The number of collisions always seems too high. Usually, much higher collision numbers were used in the measurements, so that the error can never have been greater than 10%.

Let us now discuss the second postulate. The angular distribution was

investigated for the three gases discussed here (Bibl.10) and showed no equipartition of the scattering angles. To be able to apply the diffusion theory

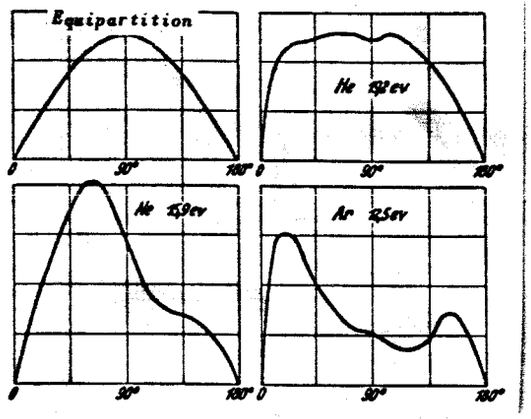

Fig.7 Angular Distribution in Electron Scattering
The ordinates give the number of electrons per zone angle.
The case of equipartition of the angles after collision
is shown in the upper left, for comparison purposes.

despite this fact, the effective cross section is replaced by the so-called diffusion cross section. The effective cross section Q_w is the sum of the effective cross sections of all atoms of 1 cm^3, at a pressure of 1 mm Hg and 0°C. The mean free path is

$$\lambda_w = \frac{1}{Q_w \cdot p}.$$

Let us now assume the atoms of the gas as being replaced by atoms produced by the equipartition after collision and let us search for the mean free path λ_d required for the electrons to obtain the same diffusion, i.e., the same density distribution and migration cross section, as in the real case. The diffusion cross section will then become

$$Q_d = Q_w \frac{\lambda_w}{\lambda_d}.$$

In the experiments made by Townsend and Bailey (Bibl.11), the diffusion /510 cross sections in inert gases were determined. However, the processing of the

data is quite complicated, so that the results cannot yet be considered fully reliable. Much more promising is the attempt to calculate the diffusion cross section from the better known effective cross sections and from the angular distributions. Kollath and Didlaukis (Bibl.12, 13) performed such calculations. For computing the migration velocities, they reduced the measured scattering angle distribution to equipartition. The result is as follows: For the diffusion, the effective cross section must be replaced by the diffusion cross section so that

$$Q_d = Q_w (1 - P).$$

Here, P is the quotient of the mean velocity vector after collision, by the velocity before collision. In the case of an equipartition, P will be equal to zero, and will be positive in forward scattering and negative in back-scattering. In general, P is determined from the angular distribution $w(\vartheta)$ by the formula

$$P = \frac{\int_0^{\pi} w(\vartheta) \cos\vartheta \, d\vartheta}{\int_0^{\pi} w(\vartheta) \, d\vartheta}.$$

In Fig.7, the angular distributions are plotted according to Ramsauer and Kollath. Using these data for converting the effective cross sections to diffusion cross sections, we will have

He at 19.2 ev: $Q_d = 0.880\ Q_w$

Ne at 15.9 ev: $Q_d = 0.815\ Q_w$

Ar at 12.5 ev: $Q_d = 0.745\ Q_w$.

Our own measurements permit a comparison of the diffusion cross sections for the three investigated gases, at least in the region of purely elastic collisions. The comparison is based on the statement that, in all gases, the collector currents become equal as soon as the product of diffusion cross section

and pressure is equal. In that case, the diffusion will be the same, which means that the losses on the inner cylinder are also equal. Consequently, if the collector current is plotted as a function of the pressure at arbitrary velocities for all three gases, these three curves can be transformed into each other on multiplying the abscissas by certain factors. The latter exactly reflect the ratios of the diffusion cross sections at these velocities. The /511 method was developed by Hertz (Bibl.14) and has been applied to argon and neon. The process becomes unreliable as soon as the electron velocities differ too much. At approximately equal velocities, however, the method is highly reliable and reproduces the ratios of the diffusion cross sections with an accuracy not lower than that of the effective cross section measurements. In our own experiments, we obtained the following values: diffusion cross section of He (18 ev): Ne (15 ev): Ar (10 ev) = 0.222:0.229:1.00.

Presumably, the error amounts to several percent. If, on the other hand, the diffusion cross sections are calculated by means of the effective cross sections given by Ramsauer (Bibl.15) and by means of the above-calculated numerical values of 1 - P, full agreement will be obtained except for the case of argon. Actually, the various measurements of the effective cross section in argon showed relatively large differences, with the slope given by Ramsauer being the highest. If, instead, a slightly lower course is selected which approaches the mean-square value of all measurements, this discrepancy will disappear.

If, then, the mean free path in the formula for the number of collisions is calculated with the diffusion cross sections and if, by means of the resultant number of collisions, the yields n are computed, then the excitation probability relative to the diffusion cross section will be obtained. (The excitation

probability must be conceived as the ratio of the excitation cross section to the collision cross section.) However, we prefer to relate the yield to the effective cross section which alone has a directly graphical meaning; for this, the η-values must be multiplied by Q_w/Q_d. It is best to include this correction immediately into the collision number formula which thus will directly yield the number of actual collisions. This formula will then read

Using the apparatus data, this produces

At 1 - P, constant values were assumed for each gas, meaning that the values obtained from the angular distributions in Fig.7 were entered. Within the narrow test range, covered by the investigations, this is no doubt justi- /512 fied. The greatest uncertainty in determining the number of collisions lies in the discrepancy of the WQ values, measured by various authors and frequently reaching 20%. Since the effective cross sections enter quadratically into the results, the effective cross section curves, used in this work, are compiled in Fig.12. They correspond to the measurements by Ramsauer, except that Ramsauer's curve for argon is lower by a factor of 0.81.

5. Determinatio[illegible]otal Yields from the Ion Current

[illegible] of total yields from a consideration of fast electrons [illegible]mit above the ionizing potential. The ions formed by electron [illegible] diffuse into the collision space and in part reach the collector, [illegible]ice the counterfield acts as an attracting field. Because of the transcon-

ductance of the counterfield through the grid, the number of ions measured will be a function of the countervoltage. The higher the countervoltage, the lower will be the ion current. In addition, the ion current as well as its course relative to the countervoltage could be a function of the pressure prevailing in the collision space. So long as the countervoltage is not sufficiently high for retaining all electrons, the ion current cannot be measured separately. Attempts to eliminate the electron current by comparative measurements led to an approximate determination of the ion current but were not sufficiently accurate for an evaluation. Consequently, it will be necessary to search for new methods to determine the yield above the ionization potential. Fortunately, such a method is provided by the ion current itself, if its dependence on the number of collisions of the electrons is considered. If the total yield η is composed of the probability for excitation α and of the probability for ionization β, the number of actual collisions n_{inel} will be

However, in this case also the number of produced ions is proportional to this function, since the effective collisions are subdivided, in accordance with the components α and β, into exciting and ionizing collisions. Consequently, the ion current will become

Here, J_s is the saturation current toward which the ion current tends with increasing pressure. Thus, the yield will be

$$\eta = \frac{1}{n} \ln (I_0 - I).$$

In Fig.8, the ion current at 18.5 ev in argon is plotted as a function of /513 the number of collisions. In all ion current measurements, the countervoltage was 30 v. The plotted curve is the pertaining calculated curve.

The test points fit well on the calculated curve and show only irregular scatterings. Specifically, the region of the saturation current shows no systematic deviations from the constant value. This has been checked, beyond Fig.8,

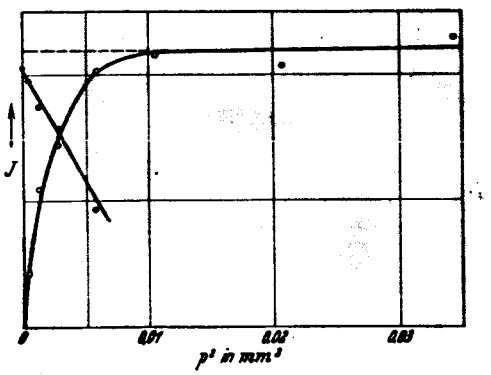

Fig.8 Ion Current as a Function of the Square of the Pressure
The straight line represents the function $\log J_0 - \log (J_0 - J)$

to a pressure of $p^2 = 0.06$. It follows from this that the ion losses during diffusion are relatively independent of the pressure. Presumably this can be explained by the fact that very small losses can be expected for ions in general. Since their kinetic energy is very low, the transconductance of the counterfield and the minor space charge fields formed by the electrons already play a role here. These fields prevent a back-scattering toward the inner cylinder, thus avoiding the losses that play such a great role in the case of electrons. Similarly, losses by recombination in the collision space are not in question here since the slow negative partners are absent. This merely leaves a loss at the outer wall of the collision space and at the grid. Even this does not depend appreciably on the pressure, and constant losses do not interfere with the results.

The accuracy of the method is approximately the same as that of the former method. Nevertheless, its use requires measurements at different pressures and, specifically, the resultant data on the general course are not more accurate

than those obtained from the absolute values. Consequently, for determining the yields in the ionization domain, we used a combination of the two methods (see Fig.9): At a given potential (the highest to which the measurement extended), the yield was determined according to the ion method. The resultant value for the current of the fast electrons, at a certain pressure, was calculated and plotted on the corresponding test curve. This made it possible, using the curve of the ion current at the same pressure, to eliminate the interfering ions in /514 the test curve and to determine the yields in accordance with the first method.

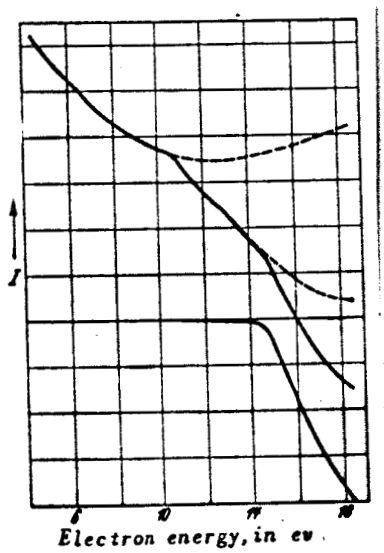

$$n_{inel} = \text{const.} \quad (1 - e^{-(\alpha + \beta)s}).$$

Fig.9 Typical Evaluation Example; Argon at 0.077 mm Pressure Solid line: top "test curve" at U = V/3; bottom, ion current curve at U = 30 v. Broken line: top "elastic curve"; bottom, slope of the test curve without ions.

So long as the domain of the measurements is not made excessively large, this constitutes the optimum method of evaluation.

6. Determination of Individual Yields

The total yields, as they had been obtained until now, constitute the sum of the excitation functions of the individual terms. Consequently, for deter-

mining the excitation functions of the terms, a subdivision of the total yields is necessary. This subdivision can be made only on the basis of countervoltage characteristics. A countervoltage curve of this type is composed of the countervoltage characteristics of the individual velocity groups that reach the collector. From this, the number of electrons of each velocity group that have reached the collector can be determined. As a typical example, let us use a countervoltage characteristic in argon at 14 ev (see Fig.3), which will give

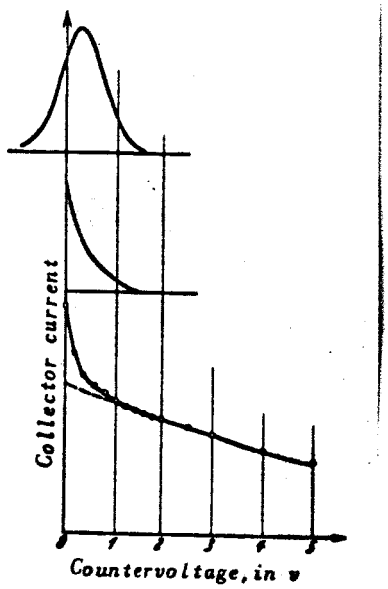

Fig.10 Elimination of the Energy Distribution of Primary Electrons

three groups: the group of fast electrons of 14 ev; one group that has lost 11.5 ev; and one group that has lost 13.1 ev. The diagram indicates that the ratio of the second to the third group is about 2.3:1. If the two groups are diffused in the collision space, under the same conditions, it follows from this that they also share in the total yield, at the same proportion.

Beyond this, the countervoltage curves permit statements on finer details of the excitation functions of individual terms which, because of the velocity distribution of the primary electrons, are less distinct in the total /515

yield. A typical example is shown in Fig.10, for helium at 20.0 ev. The diagram shows the beginning of the countervoltage characteristic; the current of the slow electrons, which had suffered an energy loss of 19.7 ev, is separated from that of the "elastic" electrons. Above this, we plotted the energy distribution of the primary electrons, shifted by 19.7 ev. This is obtained by differentiation of countervoltage curves in vacuum (see, for example, the investigations by Ramien). It is obvious that the electrons of the velocity distribution curve, located to the right of the I-axis, are able to give off 19.7 v. After the inelastic collision, they still have the volt velocity indicated by their abscissa. If the excitation probability at 19.7 ev would start abruptly and would remain constant for an additional segment, the inelastic segment of the countervoltage characteristic would have the appearance indicated at the center of the diagram. The real countervoltage characteristic deviates from this. It is obvious that its inelastic segment is formed more by very slow electrons up to 0.4 v than by faster electrons. This means that the excitation probability, 0.4 ev above the excitation potential, is much greater than at higher velocities. By tracing the countervoltage characteristics with increasing accelerating potential (the countervoltage curves were recorded always at intervals of 0.2 ev), constant check tests for such conclusions are obtained, so that reliable data can be established, specifically for the beginning of the excitation functions.

The accuracy of the data, derived from the countervoltage curves, varies widely and depends on numerous factors. Primarily, the components of the various groups of slow electrons will be erroneous if their mean free paths differ. One can attempt to eliminate this error, at least approximately, by means of current-voltage characteristics and of the known mean free paths, which has been

done in the evaluation. In addition, even minor space charges might inhibit the very slow electrons. The accuracy with respect to that of the total yields is reduced by factors of this type.

Another interference, noticeable especially in measurements with helium, is the lack of similitude of the countervoltage characteristics at various velocities and the resultant inaccuracy of the separation. This drawback is specifically great if the electrons, after the inelastic collision, still /516

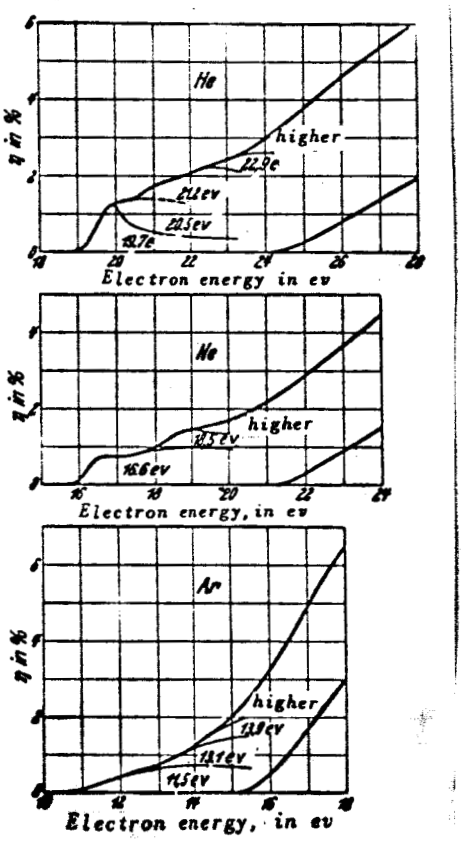

Fig.11 Total Yield and Excitation of Individual Term Groups in He, Ne, and Ar
To the right, ionization yields according to Smith.

retain a certain velocity. In that case, the proof is less reliable (the change in slope of the countervoltage curve is smaller the higher the energy of the slow electrons, at constant number), and the error becomes greater due to errone-

ous extrapolation.

If different excitation stages are close together, separation frequently becomes difficult especially in view of the fact that the countervoltage curves of the individual components, at the low velocities, are no longer similar but are influenced by the energy distribution of the primary electrons and by the form of the excitation functions. The minimum spacing of excitation stages, which still can be separated with fair accuracy, apparently is 0.7 ev. Aside from this, the uncertainty again is greatest at higher velocities.

After thus enumerating all drawbacks and possible error sources of the countervoltage characteristic method, it seems of some use to mention a circumstance that facilitates the evaluation or even - actually - often makes it possible at all. By just checking a single countervoltage curve, it would be extremely difficult or impossible to define the yield distribution. However, since we had countervoltage curves available for spacings of 0.2 v of the accelerating potential, in which - because of the width of the energy distribution - one curve always strongly overlapped the next, a running control of the obtained conclusions was possible. In addition, in the evaluation for all gases, at least two sets of plottings were used whose interpretations were widely /517 spaced in time. All of these sets showed exactly the same results, which will be discussed below. Only such curves were recorded in which the above defects could not produce excessive errors. An accuracy of about 50% does not seem overestimated.

7. Results and Discussion

Figure 11 (curves on the left) shows the results for the total yield, i.e., the sum of the excitation functions of all terms and of the ionization yield

for a single collision. (For the subdivision of the yield in Fig.11, see below.) For the collision cross sections, the effective cross sections plotted in Fig.12 were used.

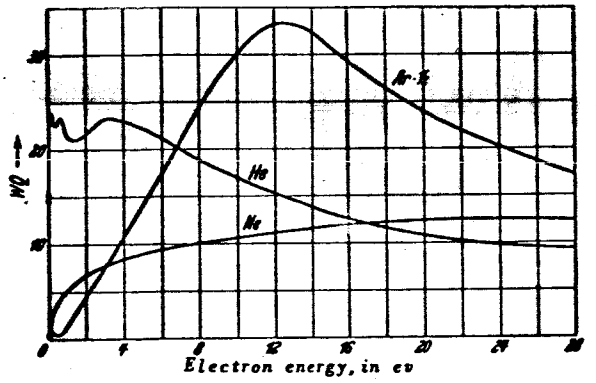

Fig.12 Effective Cross Sections Used

The velocity distribution of the primary electrons, in our measurements, had a half-width of 1.0 ev. This distribution has not been eliminated in the curves, so as not to reduce the accuracy. The mean-square error of the yields is about 20%, relative to the effective cross sections in Fig.15.

In helium and neon, the yield starts abruptly at the resonance potential and then rises gradually, with breaks at the critical potentials. Conversely, argon shows a uniform rise without distinct discontinuities. The absolute yield of the total excitation decreases from helium to argon. This leads to an even greater decrease for the excitation functions of individual terms, in view of the fact that the number of terms increases from helium to argon.

Above the ionization potential, a steeper rise occurs in all three gases. We were unable to make an exact separation of excitation and ionization yields. For this reason, the ionization probabilities according to measurements by Smith (Bibl.16) are plotted in the diagrams, whose accuracy presumably is /518 similar or greater than that of the measurements discussed here. Smith gave

the ions per centimeter path and millimeter pressure. His values were converted to collision yields, based on the effective cross section curves in Fig.12.

The discussed measurements furnish the previously lacking data for calculating the diffusion of electrons in the electric field. For example, the mean energy of the electrons in the homogeneous field, as well as the migration rate, could be calculated. Together with the measurements by Smith, this should permit a determination of the number of ionizations α.

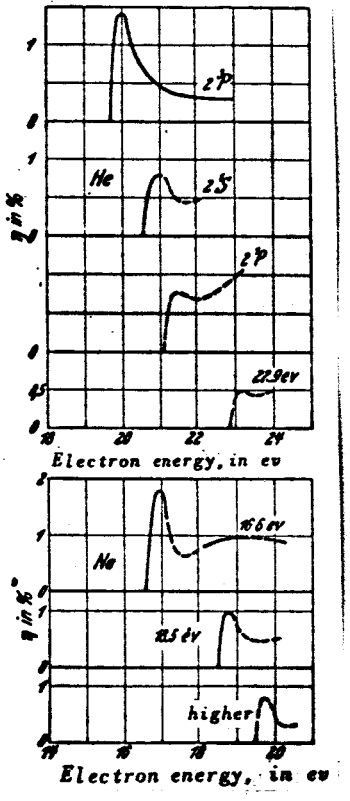

Fig.13 Excitation Functions of Individual Terms and Term Groups in Helium and Neon

The results, obtained for the excitation probabilities of individual terms, are plotted in Figs.11 and 13. Figure 11 shows the distribution of the total yield over the various components in helium, neon, and argon. Figure 13, for helium and neon, gives the results obtained after eliminating the velocity dis-

tribution of the electrons for the case of countervoltage curves. All these results, specifically those shown in Fig.13, are much less accurately defined than the total yields. For example, it is impossible to decide for the case of argon (Fig.11) whether the excitation function of the minimum jump of 11.5 ev has a maximum in the investigated region or whether it continuously and slowly rises. In Fig.13, the solid segments may be erroneous by a factor of 2, while the broken segments are even less reliable.

The most striking results are the maxima that occur in helium and neon at a few tenths volt above the excitation potential. In neon, several terms are inseparably summarized and it is impossible to define whether all have maxima. Conversely, in helium, at least the first terms are fairly well separated, and a maximum is detected on all of them. Rather interfering, at 20.5 ev ($2\,^1S$) /519 and 21.2 ev ($2\,^1P$), is the fact that the intermediate term $2\,^3P$ (20.8 ev) apparently is also excited and thus cannot be separated from the others.

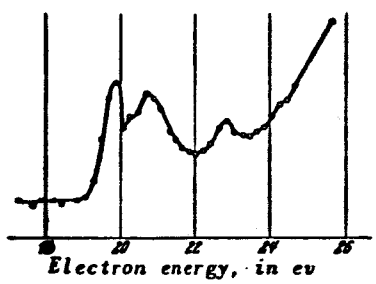

Fig.14 Hertzian Difference Curve in Helium, at 0.326 mm Pressure

Two additional means exist for detecting the occurrence of very slow electrons. Both have been used previously for demonstrating critical potentials. One of these consists in plotting current-voltage characteristics at zero countervoltage. If small space charges are present in the collision space, the presence of very slow electrons will show in a droop of the curve. (This is

true of helium, where the mean free path of slow electrons is somewhat shorter than that of fast electrons. In argon, the conditions are different.) The current-voltage characteristics, plotted during our work, show a distinct droop at 19.7, 20.6, and 22.8 ev, but none at 21.2 ev. Similar results were obtained,

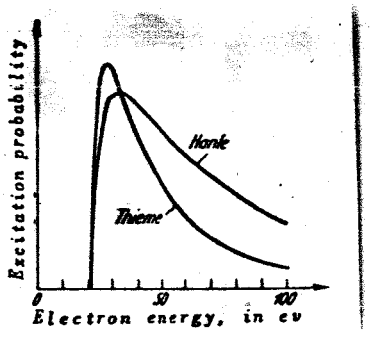

Fig.15 Excitation Function of the Line 3888 Å ($2\,^3S - 3\,^3P$) in Helium, according to Measurements by Hanle and Thieme Ordinates are not comparable.

for example, by Franck and Knipping (Bibl.17). The second method, developed by Hertz (Bibl.6), consists in measuring the slope of the countervoltage curves at the neutral point. This slope is largely determined by the number of slow electrons produced. The curve published by Hertz shows no maximum at 21.2 ev. However, it does break off at exactly this point. Later, Sponer (Bibl.18) published a curve that shows the jump distinctly at 21.2 ev. Nevertheless, there exists the possibility that space charges interfered in these measurements. If the very slow electrons are inhibited by space charges, the somewhat faster electrons will determine the slope of the curve. This explains the fact that the 21.2-ev jump is so well defined in Sponer's curve. In our investigations, such curves were also measured under conditions that presumably were only /520 little influenced by space charges; we always detected slow electrons at 19.7, 20.5, 20.8, and 22.8 ev. The 20.5 and 20.8 ev jumps were not always separate; 20.8 was stronger. Figure 14 gives a typical example of such a curve.

According to this, the excitation functions of 19.7 and 20.8 ev apparently have a strong maximum, while that of 20.5 ev has a weaker maximum and that of 21.2 ev no maximum at all in the direct vicinity of the excitation potential. This results in the following picture for the excitation functions of the helium terms, in the vicinity of the critical potentials:

The yield of the optically allowed transition $1\ ^1S - 2\ ^1P$ (21.2 ev) increases uniformly after the initial potential and, after a few volts, exceeds that of the other terms. Experiments by other authors (Bibl.19) show that, at higher potentials (about 40 v), almost exclusively the series ^1P is excited. Possibly, an insignificant yield maximum might occur between zero and 1 v above the start, but this is rather improbable.

The transition $1\ ^1S - 2\ ^1S$ (20.5 ev), which corresponds to the excitation of a quadrupole vibration, shows a yield maximum within 1 v above the excitation potential. No statements as to the further course can be made on the basis of the measurements. According to other measurements, there still is a weak excitation at 40 ev.

The intercombination jump $1\ ^1S - 2\ ^2S$ (19.7 ev) has a sharp yield maximum, approximately 0.4 v above the excitation potential, followed by a steep drop. At higher velocities, this jump is no longer excited. The transition $1\ ^1S - 2\ ^2P$ (20.8 ev) apparently shows a behavior similar to that of the previous transition. Its excitation becomes very weak, already a few volts above the critical potential.

For the higher terms of the series, excitation functions similar to the described types can be expected. Presumably, the excitation probability will decrease to less than half from one series term to the other; this can be concluded from measurements of optical excitation functions (Bibl.20).

The occurrence of a yield maximum in the vicinity of the excitation potential had frequently been detected by electrical methods. Sponer (Bibl.1), in measuring the yield in mercury, found that the metastable transition $1\ ^1S_0$ - $- 2\ ^3P_2$ has a very narrow maximum. Dymond (Bibl.5) measured the excitation /521 function $1\ ^1S - 2\ ^3S$ (19.7 ev) in helium and found a maximum very similar to that obtained by us. However, he reported the order of magnitude of the yield as being about 10 times lower. This is relatively easy to explain: Dymond used relatively high pressures and a large number of collisions. In this respect, the deceleration of slow electrons because of their shorter mean free path plays an important role, specifically since - because of the configuration of the collision space - the losses had to be large from the beginning. In addition, Dymond used rather high currents, so that minor space charges no doubt participated in increasing the losses of slow electrons.

Seiler (loc. cit.), in the transition $1\ ^1S_0 - 2\ ^1P_1$ (6.7 ev) for mercury, observed a very narrow maximum at the excitation potential. The suggestion that the excitation of metastable states has narrow maxima at the critical potential has been frequently made in the literature*. Similar results must be expected in the case of molecules. Because of the superposition of the excitation of various vibration levels, a slightly greater width will result. Maier-Leibnitz and Sponer (Bibl.21) confirmed these assumptions in their investigations on the excitation of the intercombination transition $X\ ^1\Sigma_g \rightarrow A\ ^3\Sigma_u$ in nitrogen.

No such results can be expected in investigations with optical demonstration of the excitation. This is so, since relatively high current intensities are required for obtaining measurable light intensities, so that space charges

---

* See, for example, J.Franck and P.Jordan "Excitation of Quantum Jumps by Collisions".

are unavoidable. In addition, the initial distribution of the electron energy will then become rather broad. Figure 15 shows that the results are readily influenced by such effects, specifically at the beginning of the excitation functions. One of the curves was plotted by Hanle (Bibl.22), while the second was constructed by Thieme (Bibl.20) with a similar but somewhat improved apparatus.

Michels (Bibl.23) was the only one who obtained similar maxima for all terms close to the excitation potential, in investigations of optical excitation functions in helium. He obtained the maxima by a mathematical correction applied to his results for eliminating the velocity distribution of the electrons. However, his results were extensively doubted, specifically because of the manner of his interpretation. The only reliable data are the maxima in /522 the triplets, which occur also in uncorrected curves. The information obtainable in this manner as to the position of the maxima is no better than that obtained from other optical measurements.

A comparison of these results with the theory is impossible since all available calculations, made that close to the excitation potential, are highly unreliable. Consequently, any interpretation must rely on more or less rough estimates, such as those made by Seiler. Specifically, the steep maxima at the intercombination transitions could be explained by an exchange effect. An excitation of these terms is possible only if the knock-on electron is exchanged for the atomic electron. This exchange becomes less probable the closer the velocity of the electron approaches the excitation potential, and rapidly decreases with increasing electron velocity.

In the classical theory, the transition $1\ ^1S - 2\ ^1S$ corresponds to the excitation of quadrupole vibrations. For this, a perturbation of the electron

system is required, which will become effective more promptly the longer the duration of the effect of the knock-on electron. The collision time, however, decreases with increasing electron velocity so that it can be expected that also this transition has a yield maximum at low velocities. At high velocities, the optically allowed transition $^1S - {}^1P$ is stimulated by simple excitation of dipole vibrations. This makes the gradual increase with the velocity understandable. Nevertheless, it does not seem logical that no exchange effect should take place during this transition at low velocities. The explanation lies in the fact that, in reality, an interference process rather than a simple superposition of different excitation processes is involved. This makes it extremely difficult to make any theoretical statements as to the magnitude of the effects under different conditions.

8. Supplement

In a recently published paper, Löhner (Bibl.24) reported on results obtained with still another method. His procedure permits a much better separation of the excitation of individual terms. However, he made measurements in each gas at only one electron velocity, so that no statements can be made on the general course of the excitation functions. In addition, the values for the total yield, given by Löhner, are much higher than ours. Of course, agreement cannot be expected here, since Löhner considered only electrons deflected through relatively low angles, whereas - in the case of multiple collisions - all angles are uniformly included. At higher velocities, it is a frequently observed fact that the elastic scattering is much more uniform than the in- /523
elastic type. Inelastic scattering is more restricted to low angles. If the same were the case at low velocities, the yields measured by Löhner would have

to be higher than ours.

9. Summary

The total yield at collisions of slow electrons in helium, neon, and argon is determined by two methods.

First method: Electrons of known velocity enter a gas-filled field-free collision space and scatter there. A part of the electrons reaches a collector. By applying suitable countervoltages between collision space and collector, it is possible to permit only electrons that had received no energy by inelastic collisions to reach the collector. Thus, the collector current is weakened by a) loss of electrons due to lateral diffusion and back-scattering; b) inelastic collisions. The losses (a) can be determined by comparative measurements below the resonance potential. The losses (b) can be used for determining the excitation probability, provided that the number of collisions is known.

Second method: Above the ionization potential, ions are produced in the collision space of which most reach the collector and make an application of the first method impossible. Here again, consideration of the ion current alone (high countervoltage!) and its dependence on the number of electron collisions permits determining the yield.

The obtained results on total yields are practically free of instrument errors, such as those produced by electron reflection at the metal parts, anomalities of the effective cross sections, angular distribution during scattering, minor space charges, and similar factors. The accuracy is about 20%. By making use of Smith's measurements on the ionization probability, a separation of excitation and ionization yield is obtained. This furnishes all data required for studying the motion of slow electrons in the electric field within

these gases.

By considering countervoltage curves in a manner similar to that used, for example, by Seiler, it becomes possible to obtain at least a partial and qualitative subdivision of the total yield into the excitation functions of individual terms (see Fig.13). The main result here is that sharp maxima of the excitation functions are frequently detected in the direct vicinity of the initial potential.

Our work has been performed at the Second Physical Institute of the University Göttingen. We wish to express our thanks to Prof. Dr. J.Franck for suggestions and continuous support. Appreciation is expressed also to the staff members of the Institute.

BIBLIOGRAPHY

1. Sponer, H.: Z. Physik, Vol.7, p.185, 1921.
2. Seiler, R.: Z. Physik, Vol.83, p.789, 1933.
3. Harries, W.: Z. Physik, Vol.42, p.26, 1927.
4. Ramien, H.: Z. Physik, Vol.70, p.353, 1931.
5. Dymond, E.G.: Proc. Roy. Soc. London, Ser.A, Vol.107, p.291, 1925.
6. Hertz, G.: Z. Physik, Vol.18, p.307, 1923.
7. Hertz, G.: Z. Physik, Vol.32, p.298, 1925.
8. Bartels, H. and Nordstrom, C.H.: Z. Physik, Vol.68, p.42, 1931.
9. Harries, W. and Hertz, G.: Z. Physik, Vol.46, p.177, 1927.
10. Ramsauer, C. and Kollath, R.: Ann. Physik, Vol.12, p.529, 1932.
11. Townsend, J.S. and Bailey, V.H.: Phil. Mag., Vol.42, p.873, 1921; Vol.43, pp.93, 127, 1922; Vol.44, p.1033, 1922; Vol.46, p.657, 1923.
12. Kollath, R.: Ann. Physik, Vol.15, p.485, 1932.

13. Didlaukis, M.: Z. Physik, Vol.77, p.352, 1932.

14. Hertz, G.: Physica, Vol.2, p.87, 1922; Proc. Amsterdam, Vol.25, p.90, 1922.

15. Ramsauer, C.: Jahrb. Radiol., Vol.19, p.345, 1922.

16. Smith, P.T.: Phys. Rev., Vol.36, p.1293, 1930.

17. Franck, J. and Knipping, P.: Z. Physik, Vol.1, p.320, 1920.

18. Sponer, H.: Z. Physik, Vol.18, p.249, 1923.

19. McMillen, J.H.: Phys. Rev., Vol.36, p.1034, 1930.

20. Thieme, O.: Z. Physik, Vol.78, p.412, 1932.

21. Maier-Leibnitz, H. and Sponer, H.: Z. Physik, Vol.89, p.431, 1934.

22. Hanle, W.: Z. Physik, Vol.56, p.94, 1929.

23. Michels, W.C.: Phys. Rev., Vol.36, p.1362, 1930.

24. Löhner, H.: Ann. Physik, Vol.22, p.81, 1935.

Received May 7, 1935